Frontiers in Audiology and Otology

First *in vivo* test of a biodegradable polymeric stent for the Eustachian tube in sheep

Stina Winkelmann[1], Kerstin Lebahn[2], Malena Ezzat[1], Katharina Schmitt[1], Alexandra Napp[1], Niels Oppel[1], Friederike Pohl[1], Andreas Kampmann[3], Niels Grabow[2], Thomas Lenarz[1,4] and Gerrit Paasche[1,4]*

[1]Department of Otorhinolaryngology, Hannover Medical School, Hannover, Germany, [2]Institute for Biomedical Engineering, Rostock University Medical Center, Rostock, Germany, [3]Department of Cranio-Maxillo-Facial Surgery, Hannover Medical School, Hannover, Germany, [4]Cluster of Excellence Hearing4all, Hannover Medical School, Hannover, Germany

Introduction: Eustachian tube dysfunction can cause inadequate ventilation of the middle ear and is therefore one of the main reasons for the development of chronic middle ear infections. This can significantly impact the quality of life. There is a variety of treatment options, but in most cases long-term success is limited. For this reason, stenting the Eustachian tube (ET) may be a safe and effective alternative. Biodegradable stents have been developed that support the impaired ET function until natural ventilation of the middle ear via the ET is restored, and dissolve after their function has been fulfilled.

Objective: The purpose of the current study was to investigate feasibility of implantation and degradation kinetics of biodegradable polymer stents in the ET.

Study design: The study was set up as an orientation study.

Methods: Biodegradable stents (diameter: 3.5 mm; length: 15 mm) were made from Poly-L-lactic acid (PLLA) in a dip-coating process and subsequent laser cutting and were crimped on a balloon catheter. Stent implantation into the ET was performed unilaterally in nine healthy female blackface sheep under endoscopic control with a dedicated insertion tool and an inflation pressure of 10 bar for 2 min. Ventilation of the middle ear was controlled by tympanometry weekly throughout the observation period of 3, 6, or 12 months (three animals each). After the final examination, cone beam computed tomography scans and histological examinations of the ETs were performed.

Results: All stents could be inserted as planned. Pharyngeal orifices of all sheep were closed at half-time and final follow-up inspections. After 3 months, all stents were functional, but already showed first fragment formation. Six months after insertion, the stents had largely collapsed but still held open a residual lumen and after 12 months, the ETs were completely collapsed close to their natural shape. Fragments of various sizes were found distributed in the tissue beneath an epithelialized ET.

Conclusion: The polymeric ET stent can be reliably positioned without generating a patulous ET. It seems to support ET function for about 3 months before functionality is lost.

KEYWORDS

Eustachian tube dysfunction, middle ear ventilation, otitis media, polymeric stent, sheep as an animal model

1 Introduction

Otitis media with effusion (OME) is a disease that is particularly common in children and is typically related to Eustachian tube dysfunction. Also about 1% of the adult population is affected by chronic Eustachian tube dysfunction (Di Martino et al., 2004).

The Eustachian tube (ET) plays an essential role in the pathogenesis of otitis media (Healy and Rosie, 2003). This is due to the anatomical and physiological relationship with the middle ear (Bal and Deshmukh, 2022). The functions of ET are diverse. The main functions include pressure equalization and ventilation of the middle ear (Goulioumis et al., 2022). In addition, the ET serves the mucociliary clearance of secretions from the middle ear, as well as protecting the middle ear from loud sounds and from nasopharyngeal secretions and pathogens (Schilder et al., 2015).

The ET is closed for most of the time. A short active opening through activation of paratubal muscles is possible while swallowing or other maneuvers e.g. for pressure equalization (Teixeira, 2020). If this system is disrupted by inflammation, compression of the lumen or a collapse of the ET or dysfunction of the involved muscles, this can lead to ET closure (Schrom et al., 2007). In the event of a functional failure, Eustachian tube dysfunction (ETD) occurs (Schilder et al., 2015). Consequences can include acute and chronic otitis media, conductive hearing loss and even cholesteatoma (Miller et al., 2014).

There are various treatment options available today. Conservative measures, including the Valsalva maneuver to equalize pressure, nasal douching with saline solution and the application of decongestants, corticosteroids and antihistamines in the nasal passages can be used (Pohl et al., 2018).

Conventional surgical procedures for ETD involve the myringotomy and the insertion of a tympanostomy tube into the tympanic membrane (Bal and Deshmukh, 2022). Middle ear pressure can be equalized, and fluid can be drained. However, using this approach, symptoms are primarily treated. Conventional treatment with tympanostomy tubes carries the risk of eardrum perforation and therefore conductive hearing loss (Bal and Deshmukh, 2022) and leads to a reduction in quality of life (e.g. restrictions for swimming). Other mechanical interventions include Laser tuboplasty for the removal of enlarged mucous membranes (Poe et al., 2007), as well as Balloon Eustachian Tuboplasty (BET) (Sudhoff et al., 2013). BET as a minimally invasive procedure shows a success rate of 36%−80% (Silvola et al., 2014; Williams et al., 2016). However, not all patients respond to this treatment method. Therefore, more treatment options are needed.

One research approach is the implantation of stents into the Eustachian tube. The clinical use of stents is known from other areas of medicine. Stenting of arteries in cardiovascular medicine is routinely performed with stents manufactured from for example CoCr, stainless steel and NiTi (Beshchasna et al., 2020). Biodegradable alternatives for coronary arteries already exist and are part of further research (Hu et al., 2018). Biodegradable stents are also being used clinically in the gastrointestinal area, for example in the treatment of esophageal diseases (Kang, 2019). The aim of stent application in the ET is to restore ventilation of the middle ear without generating a patulous ET. Cadaver studies have shown that blackface sheep are an anatomically suitable model for preclinical investigations of stents intended for human use due to similarity of the ET to humans (Miller et al., 2014). Feasibility of stent implantation in the ET *in vivo* has already been successfully demonstrated in sheep and pig models (Pohl et al., 2018; Kang et al., 2022a). In addition, the tympanometry method for investigating middle ear ventilation was successfully adapted to the use in conscious sheep (Pohl et al., 2017) to provide information about tympanic membrane integrity, middle ear ventilation and thus ET function. Further investigations in human donor bodies showed that stents made from Nitinol (NiTi) seemed to adapt better to the shape of the ET than cobalt chromium (CoCr) and polymeric stents (Rosenbusch et al., 2023). This investigation also indicated that tubal anatomy should be taken into account for the development of an ET stent.

An essential part of the previous studies on this topic was supporting the ET through permanent stents. However, the needs of patients differ and not everyone requires permanent support of the ET. In this case, biodegradable stents would be preferable. First tests with absorbable magnesium stents in a porcine model showed a good biocompatibility but the material degraded rapidly, and functionality was lost within 2 weeks after implantation (Kang et al., 2023). A first stent prototype made from poly-L-lactic acid (PLLA)-based polymeric blend was investigated in the ET of human donor bodies (Rosenbusch et al., 2023). In addition, biodegradable polymer stents were already used in clinical application for other purposes (Ailianou et al., 2016).

Prototypes of biodegradable polymer stents in the current study were designed to restore impaired tubal function and degrade slowly, to give a temporary support. According to the ENT surgeons involved, a stent should maintain ventilation of the middle ear for about 3 months to enable healing of any existing inflammation. The purpose of the current study was to investigate feasibility of implantation and degradation kinetics of biodegradable polymer stents in the ET. The study was set up as an orientation study. The biodegradable polymeric stents were implanted in the Eustachian tube of sheep for different observation periods to investigate implant functionality, i.e. the time the stents keep their round shape and the ET widened, and degradation behavior in the ET environment.

2 Materials and methods

2.1 Ethic statement

All *in vivo* experiments in this study were conducted in accordance with the German and European Animal Welfare legislation. They were approved by the State Office for Consumer Protection and Food Safety, Department of Animal Welfare under the number 20/3531. The experiments were performed with regards to the valid directives regarding accommodation, usage and care of experimental animals. The sheep were accommodated in the Central Animal Facility (CAF) of Hannover Medical School.
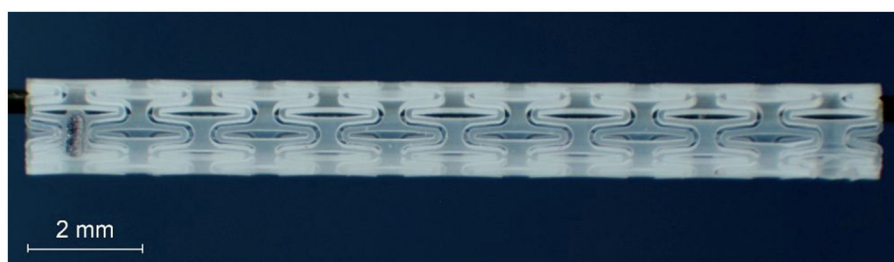
FIGURE 1
Laser cut polymeric Eustachian tube stent with integrated radiopaque marker before crimping.

2.2 Stents

Biodegradable polymer stents (Figure 1) were developed and fabricated at the Institute for Biomedical Engineering of the Rostock University Medical Center. They were made from Poly-L-lactic acid (PLLA) in a dip-coating process and subsequent laser cutting with a patented stent design (Schümann et al., 2016). The stents had a length of 15 mm and a nominal diameter of 3.5 mm. Each stent was equipped with two tantalum X-ray markers at the end of the stent with a distance of 13 mm and a rotation around the circumference of 60°. For insertion, the stents were crimped on a standard cardiovascular balloon catheter (3.5 × 15 mm). Further technical information is provided in Schümann et al. (2018, 2020).

2.3 Animals and study design

The experiment was conducted with nine healthy female adult (2–4 years) German black headed meat sheep, also named blackface sheep.

The experimental procedure (see also Supplementary Figure 1) started with taming and training for 4 weeks. After 1 week of taming, a gradual introduction into the steps to carry out tympanometric measurements on awake animals followed. Every 2–3 days the health status was checked. After general anesthesia (GA), it was checked at higher frequency.

In week −1, the external ear canal (EAC) was cleaned under GA. In addition, the pharynx and both pharyngeal ET ostia were inspected endoscopically for regular anatomy. The sheep were implanted unilateral in week 0 with $N = 3$ per group. The side to be implanted was chosen according to a randomization protocol. Sheep P1–P3 were observed for 12 months, P4–P6 for 6 months and P7–P9 for 3 months. This study was set up as an orientation study. For this reason, a small number of animals were chosen. Therefore, no statistical evaluation was possible.

At half-time control (after 6 months, 3 months and 6 weeks, respectively) and final control endoscopic examinations of EAC, the tympanic membrane and the Eustachian tube ostia were performed under GA and documented.

Tympanometric measurements were conducted in week −1 and week 0 to ensure a ventilated middle ear before stent insertion. Subsequently, regular tympanometric measurements were performed once a week to monitor middle ear ventilation status.

At the end of the period, samples from the Eustachian tube were collected and evaluated histologically.

2.4 Cleaning of the external ear canal

The first mechanical cleaning of the EAC took place 1 week before stent implantation under GA following the protocols of Oppel et al. (2022a) and Pohl et al. (2017). The aim was to remove earwax obstructions and to enable correct tympanometric measurements. Sedation was achieved using midazolam (0.2 mg/kg i.v.; Midazolam-ratiopharm 15 mg/3 ml, ratiopharm GmbH, Ulm, Germany). The GA was induced with propofol (5–10 mg/ml i.v.; Narcofol® 10 mg/ml, CP-Pharma GmbH, Burgdorf, Germany) and maintained with isoflurane (1.5%–2.0% end-tidal inhalation; Isofluran CP® 1 ml/ml, CP-Pharma). Postoperatively, pain treatment was administered with carprofen (2 mg/kg i.v., Carprosol® 50 mg/ml, CP-Pharma). Mechanical cleaning was performed otoscopically (KILLIAN-STRUYCKEN nasal speculum 55 mm, KARL STORZ SE & Co, Tuttlingen, Germany). Larger accumulations of earwax were removed from the EAC with looped probe under endoscopic control (WEBER-LOCH ear loop size 1, Karl Storz). A rigid endoscope (HOPKINS® 70°, 4 mm in diameter, 30 cm in length; KARL STORZ SE & CO.KG, Tuttlingen, Germany) was used for all endoscopic checks during the experimental period. It was attached to a telecam PAL (KARL STORZ) and connected to a Tele Pack Vet X LED RP 100 system (KARL STORZ). Smaller accumulations of earwax were dissolved using Otodine® (main ingredients: prophylenglycol, chlorhexidingluconat, pH 8 Tris-EDTA; aniMedica, Senden-Bössensell, Germany) under visual control. After cleaning, the EAC and the tympanic membrane were examined endoscopically for any abnormalities. Throughout the entire experimental period, the EAC was flushed with Otodine® once a week to prevent the accumulation of earwax. During all following GA, visual checks and, if necessary, mechanical cleaning of the EAC were carried out.

2.5 Tympanometry

Tympanometric measurements were conducted to monitor middle ear pressure in conscious sheep. These measurements were performed using a commercial handheld tympanometer (Madsen

Otoflex 100, GN Otometrics, Münster, Germany) using the method of Pohl et al. (2017). The tympanometer operated with a probe tone of 226 Hz. The pressure changed (500–600 daPa/s) from positive to negative as quickly as possible, with a maximum range of −400 to 200 daPa. To obtain reliable data, three consecutive measurements were taken per ear in a quiet environment. Due to the sheep's long and angled outer ear canal, a special adapter (Pohl et al., 2017) was used to position the probe in the bony part, allowing for proximity to the tympanic membrane. It was composed of a polyurethane tube (PUN-6 x 1, Festo AG & Co KG, Esslingen, Germany) attached to the connector of a KimVent Microcuff Endotracheal Tube (Kimberly-Clark, Roswell, NM, USA). To fully seal the Eustachian tube, a red tip of 10 mm size (GN Otometrics) was used.

Tympanograms were classified into different curve types based on Gelfand (2016). A type A tympanogram depicts a physiological middle ear status with balanced pressure in the tympanic cavity and therefore a functioning Eustachian tube. Type B does not have a clear peak or has a flat course. Tympanic membrane perforation, tympanic effusion or a blocked probe due to earwax accumulations are possible causes for this. The reasons can be differentiated by measuring the ear canal volume (ECV). It is normal with OME, significantly reduced in the case of earwax accumulations and increased in the case of perforations. A type C tympanogram shows a non-physiological pressure in the middle ear and indicates tubal dysfunction. It is generally shaped like a type A tympanogram, but the maximum is shifted into the negative pressure zone by more than 100 daPa.

2.6 Stent implantation

Stent implantation took place under GA as described under 2.4. To prevent bleeding and to provide local anesthesia, pointed swabs soaked with 5 ml of Lidocaine (Xylocitin®-loc 2%, mibe GmbH, Brehna, Germany) and 10 ml of xylometazolinhydrochloride (Otriven 0.1%, GlaxoSmithKline Consumer Healthcare GmbH & Co. KG, Munich, Germany) were applied into the nostrils for 5 min.

The anatomical situation of the nasopharynx was inspected via endoscope. It was inserted through the ventral nasal meatus on the opposite side of the desired ET opening. The viewing angle of 70° was directed toward the side and the optic was moved forward, closely following the inferior turbinate until the ET opening was seen. Next, the endoscope was moved sideways to position it in front of the opening and rotated to view the orifice from the side.

Via the other nostril, a stent application instrument prototype (bess Medizintechnik, Berlin, Germany) with flexible tip was introduced into the nasopharynx. The stent on the balloon catheter was advanced through the tool into the ET. The balloon was filled with saline solution. Applying a pressure of 10 bar for 2 min, the stent expanded. After that, the balloon was deflated and kept in place for 1 min before it was slowly removed from the ET opening.

2.7 Cone beam CT scans

Cone beam computed tomography (CBCT) scans (3D Accuitomo XYZ Slice View Tomograph, J. MORITA MFG. Corp.,

Kyoto, Japan) of the sheep head were made directly post mortem. After embedding the samples for histology (see below) CBCT images were taken (XCat; Xoran, voxel size 0.4 mm, Ann Arbor, MI, USA) again. The X-ray markers were used as an orientation to locate the stents in the samples.

The images were loaded into 3D Slicer (version 5.0.3) software (https://www.slicer.org, accessed on August 5th, 2022) to generate a 3D dataset of the ET and anatomical structures (Federov et al., 2012).

2.8 Fixation, embedding and staining procedure

On the day of the final inspection after 3, 6, or 12 months of implantation, euthanasia took place under GA by an overdose of Pentorbital i.v. (Release® 300 mg/ml, WDT, Garbsen, Germany). Decapitation behind the second cervical vertebrae followed and CBCT scans were taken.

To prepare the tube for histologic analysis, first each ET with surrounding tissue was dissected using a bone saw (FK23 bone saw, Bizerba, Balingen, Germany).
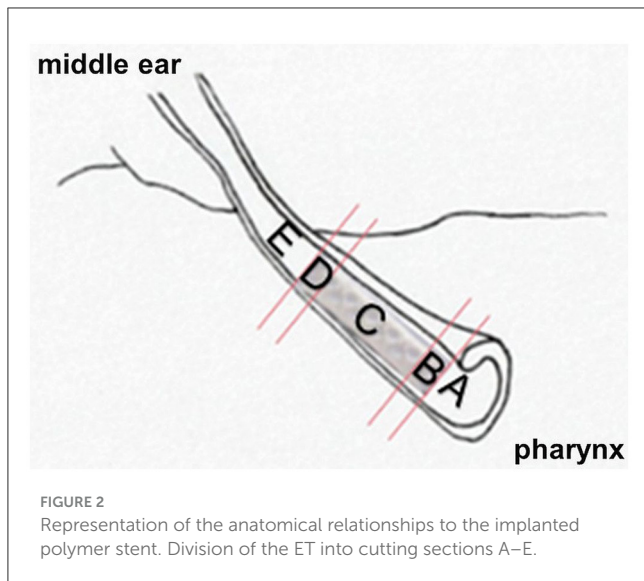
Next, the samples were fixed in formaldehyde (4%, stabilized, phosphate buffered; CHEMSOLUTE, TH. GEYER GMBH & CO. KG, Renningen, Germany) for a total of 3 weeks with changing the solution twice a week. After each change, vacuum was drawn for 10 min. After fixation, the samples were washed in phosphate-buffered saline (PBS; PBS tablets dissolved in destilled water; Gibco, Schwerte, Germany) for 4 h.

Dehydration via increasing ethanol series (Carl Roth, Karlsruhe, Germany) followed. It started with 70% ethanol, then 80% ethanol and 90% ethanol, with each step being carried out for 48 h with an ethanol change after 24 h. This was followed by 100% ethanol, 100% ethanol—acetone 1:1, pure acetone and absolutely undenatured ethanol for 24 h each. After each change, vacuum was drawn, except when acetone was included in the step.

Then the samples were preinfiltrated with pure methylmethacrylate (MMA; Merck KGaA, Darmstadt, Germany) for ∼24 h and again vacuum was drawn. The next day a mixture of methylmethacrylate, benzoyl peroxide (with 25% H_2O for synthesis; Sigma-Aldrich Chemie GmbH, Taufkirchen, Germany) and triacetin (EMPROVE® ESSENTIAL Ph Eur, BP, USP; Sigma Aldrich) was added. Polymerization of the sample took place in a water bath at about 37.5°C for 2–4 days. Excess MMA was removed from the specimen using a plaster model trimmer (HSS 88, Wassermann Dental-Maschinen GmbH, Hamburg, Germany).

The specimen were cut into two halves and then fixed onto specimen holders. Using a saw microtome (Leica SP1600®, Leica Biosystems, Wetzlar, Germany) slices of approximal 45 μm thickness were cut under water-cooling. The cutting sections on the stent side were divided in A (region before stent as seen from pharynx), B (beginning of stent), C (middle of stent), D (end of stent) and E (behind stent; Figure 2). The slices started in the middle of each ET and followed the course of the ET in both directions. Five slices were made per stent section. On the control side in total three histological slices were made from the middle part of the cartilaginous part of the ET. Cover glasses were attached to

FIGURE 2
Representation of the anatomical relationships to the implanted polymer stent. Division of the ET into cutting sections A–E.

FIGURE 3
(A) Cross section of an ET without stent (animal P7). Depicted are glandular tissue (G), epithelium (E), free lumen (L_F), tubal cartilage (C) and bone (B). **(B)** Cross section of the ET of sheep P4 with stent in cutting section C. The tubal lumen (yellow), the secretion in the tube lumen (green), the stent area (blue) and the quadrant formation for epithelial evaluation (red) with the quadrant division (1–4) are shown as examples according to the evaluation procedure.

the clean, dry cut surface using super glue (Instantbond Klebstoffe GmbH, Berlin, Germany).

Slices were stained using Löfflers Methylene blue (ready solution; Merck) and Alizarin red S (Alizarin red S staining solution; Merck). Methylene blue was heated up to 75°C and after reaching temperature, the slices were stained for 10 s. After rinsing with tap water and letting them dry, the slices incubated for 90 s in Alizarin red S at room temperature. For this step 0.5 g Alizarin red S were solved in 45 ml bidistilled water and 5 ml of ammonia solution. Again, a rinsing step followed. The slices were stored between dry block paper and clamped in a press. Slices dried in an incubator at 37°C overnight. After these steps, each slice was attached on microscopic slides with Entellan Neu® (Merck) and then covered with cover slips.

2.9 Histologic analysis and evaluation

Histologic analysis was performed using the BZ-II-Viewer program after digitization with the Keyence BZ-9000E microscope (KEYENCE DEUTSCHLAND GmbH, Neu-Isenburg, Germany).

At $2\times$ magnification, the entire histological section was assembled from individual images to form an overview image. The number of individual images varied depending on section size and position. At $4\times$ magnification, the area of the tube was imaged such that the tube and stent were completely depicted. All histological evaluation was carried out using the $4\times$ images (Figure 3A).

On the control side, a total of three representative histological slices from the middle portion of the cartilaginous part of the ET were evaluated per animal (Figure 3A). On the stented side, three slices were analyzed in each section (A–E), resulting in 15 analyzed slices per animal. If possible, the histological slices were selected sequentially in each section.

In each slice, the lumen of the ET (L), the amount of secretion in the tube lumen (S), the area of the stents (A), the number of visible struts and the integrity of the epithelial lining (E) were analyzed (Figure 3B).
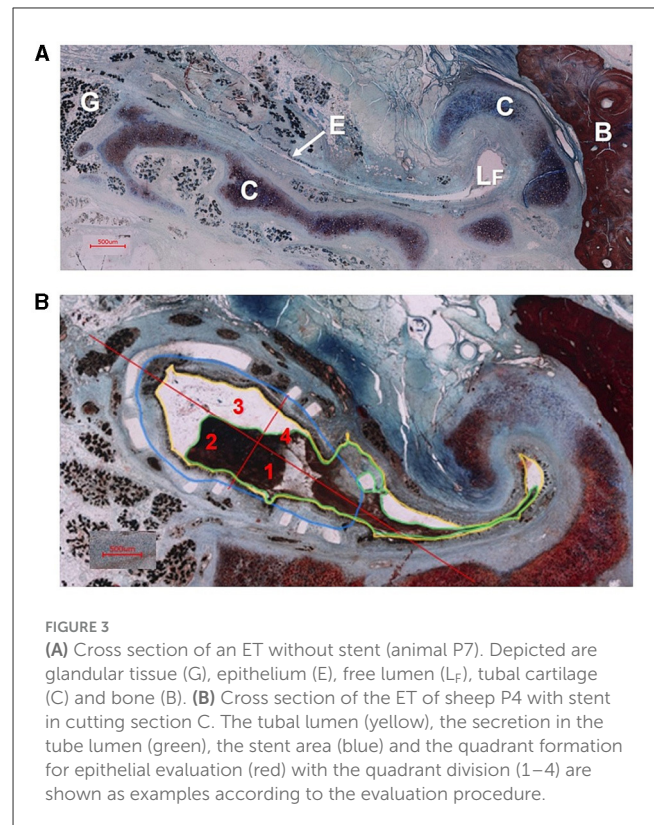
The lumen (L) of the Eustachian tube was determined by a line drawn at the boundary between the epithelium and the lumen (compare Figure 3B). The complete lumen of the ET was measured both within and outside the stents, including struts within the lumen.

The secretion in the entire tube lumen (S) was measured in all slices on the control side and all cutting sections (A–E) of the implanted side. Struts surrounded by secretion were counted as part of the secretion. The area of the stent (A) was considered in cutting sections B–D on the stent side. Individual struts deviating significantly from the expected position were not taken into account. To determine the area of the stent, the struts were connected along their inner edge.

When counting the visible struts, a distinction was made between the total number of visible struts and the free struts located exclusively in the tube lumen. Results were averaged for each cutting section (A–E) in each animal before mean values for treatment groups (P1–3, P4–6, P7–9) or the entire stent of an animal were calculated.

The assessment of the epithelium involved dividing the stent area (cutting sections B–D) into four quadrants on each slice. One line ran through the transition to the tubal lumen in the hook area outside the stent area and a second one ran orthogonal to this line (Figure 3B). Each quadrant was evaluated separately. On the control sides, only one value was assessed per slice. The evaluation was rated from 1 to 4 with 1 standing for mostly intact epithelium (> 80%), 2 for partially intact (20–80%), 3 for not intact (< 20%) and 4 for no available epithelium. No available epithelium in this

TABLE 1 Score of ET opening for each sheep.

	P1 r	P2 l	P3 r	P4 l	P5 l	P6 r	P7 r	P8 l	P9 r
SI	1–2	1	1	1	0	1	1	0	1
HT	0	0	0	0	0	0*	0	0*	0
Final	0	0	0	0	0	0	0	0	0

The score was collected during stent implantation (SI), half-time check (HT) and final check (Final) through endoscopic control under GA for each animal (P1-P9). Left (l) and right (r) indicate the stented and therefore displayed side. 0—ET closed; 1—ET minor opening; 2—ET moderate opening; 3—ET profound opening.
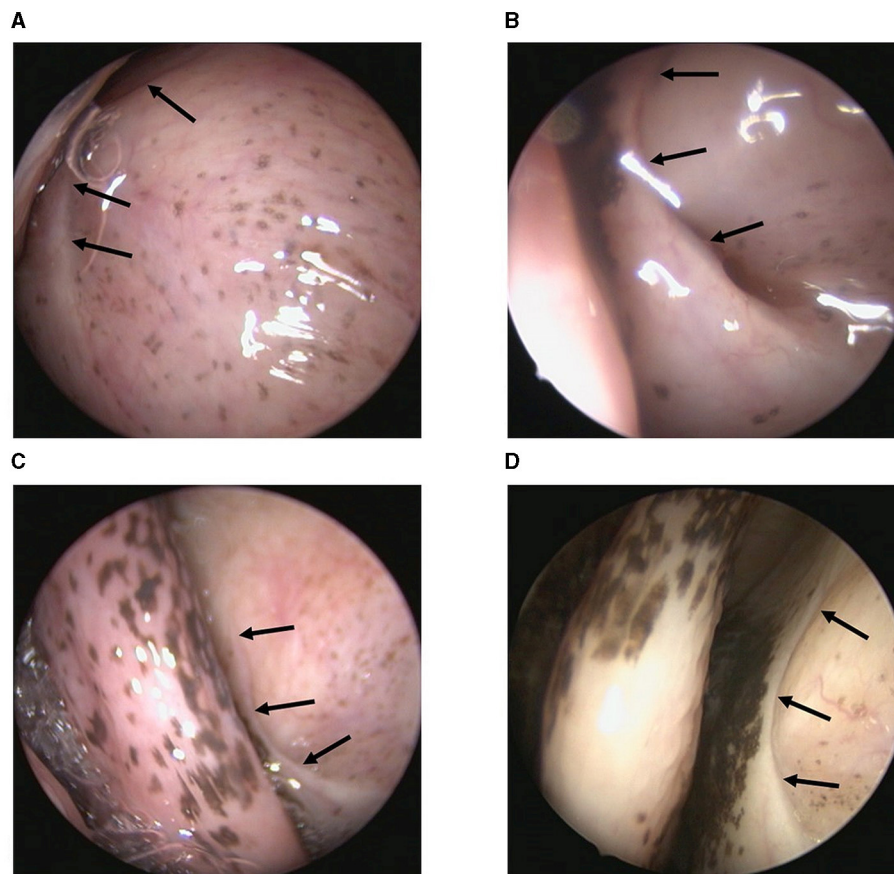*Mucus detectable at ET entrance.

FIGURE 4
Endoscopic view of nasopharyngeal ET entrance of sheep P2 at different points in time. (A) Before stent implantation, (B) Directly after stent implantation, (C) Half-time check and (D) Final control are shown. The arrows point to the ET entrance, which is usually closed.

case meant that the entire quadrant was filled with tissue and no epithelium (independent if damaged or not) was detected.

3 Results

Implantation of the polymeric stents in all nine sheep proceeded under endoscopic control without complications. The stents were positioned as desired. During regular veterinary exams, the sheep showed no change in clinical health status or signs of discomfort. All treatments under general anesthesia were well tolerated. Additionally, the tympanometric measurements on the awake animals were successfully conducted.

3.1 Endoscopy

All animals had closed tube entrances during the first endoscopic check. As shown in Table 1, endoscopic controls immediately after stenting showed that seven out of nine sheep had a minimal opening of the nasopharyngeal orifice (compare also Figure 4). The remaining two sheep had closed tube entrances even immediately after stent insertion. The half-time and final checks revealed closed ET entrances in all animals. Two animals (P6, P8) showed temporary mucus formation in front of the entrance of the ET, which disappeared until the final checks.

Examinations of the ear canal and eardrum showed no signs of inflammation or other pathological abnormalities (Figure 5).
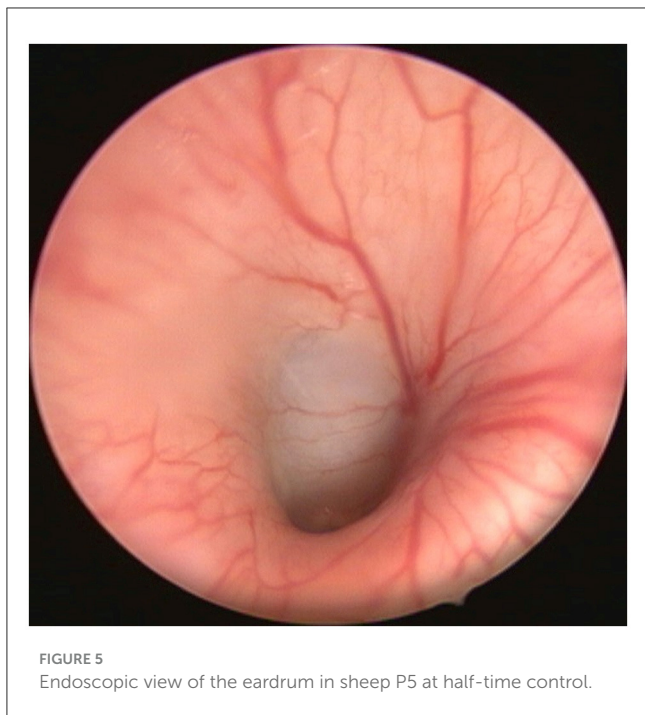
FIGURE 5
Endoscopic view of the eardrum in sheep P5 at half-time control.

TABLE 2 Results of tympanomeric measurements.

	Stent	Control
P1 r	Always A	B: w3, 5–7, 12, 14, 20, 22, 26, 30, 31–33
P2 l	C: w6, 38	B: w33
		C: w39, 44, 49
P3 r	B: w5, 7, 9, 10, 27–39, 45	B: w32, 35
	C: w6, 26, 42, 46, 49	
P4 l	B: w1, 5, 6, 15, 19, 20, 22, 25, 26	Always A
	C: w0	
P5 l	C: w8, 11, 23	C: w17, 22
P6 r	B: w4–26	B: w18
	C: w−1, 0, 3	C: w9, 11
P7 r	Always A	B: w0
P8 l	C: w4	Always A
P9 r	C: w7, 12	Always A

Measurements were conducted in triplicate. If at least two out of these three measurements yielded similar results, they were deemed reliable. Explanation of the classification options: A—Physiological curve type, B—Pathological flat curve type, C—Pathological curve type (shifted into negative pressure). Only weeks (w) with curve types B or C are provided. All other measurements indicated a ventilated middle ear (type A). The gray highlighted values indicate the prolonged ventilation disorders.

P1 already had an irregular surface and redness of the eardrum before stenting, but the redness disappeared during the experiment. Cleaning of the EAC due to ear wax obstruction was necessary in all cases at the GA before stent implantation. In addition to the weekly rinsing with Otodine®, mechanical post-cleanings of the EACs were needed in the subsequent endoscopic examinations during stenting for P2 (right side), P4 (right), P6 (right), during half-time check for P7 (left), P9 (right), and during final check for P6 (right), P7 (left) and P8 (left).

3.2 Tympanometry

Tympanometric measurements on the awake animals were successfully conducted. Two animals (P3, P6) showed prolonged ventilation disorders developed on the stent side during the observation period (Table 2). In both cases, the ventilation disorder developed several weeks after stent implantation. In P3 the ventilation disorder disappeared over time, in P6 it remained until euthanasia.

Exclusively type A tympanograms were measured on the stented side in two animals (P1, P7) and on the control side in three animals (P4, P8, P9). All other ears (implanted and not implanted) showed sporadic short-term ventilation problems. These ranged from one to three measurements (weeks) in a row.

3.3 Cone beam CT

A differentiated evaluation of the CBCT images of the heads was carried out using the X-ray markers (Figure 6). Originally, each implanted stent was equipped with one X-ray marker at each end, as the stents themselves are not visible in the CBCT. In seven cases,

only one X-ray marker was found. In the case of P8, a 3-month stented sheep, both markers were still present, while one 6-month stented animal (P6) no longer had any X-ray marker. In this case, air was found where the stent should be positioned (Figure 6A).

Based on the position of the marker in relation to the tube entrance and the bony part of the ET, it can be assumed that always the marker close to the middle ear remained in place.

3.4 Histology

The histological processing was successfully completed for all sheep. Example images for all three groups can be found in Figure 7. General observation was that after 3 months, some fragmentation of the stent could be seen, but it still expanded the ET and the struts were predominantly circular arranged. After 6 months, degradation had progressed and the strut arrangement deviated clearly from its original shape. Twelve months after implantation, the stent had collapsed but only in one case (P1) the ET has returned to its natural shape. For this reason, not all intended measurements could be carried out for all slices of all stents.

The lumen (L) area of the ET was assessed in the histologic analysis. Examination of the lumen on the control side resulted in an average value of 0.80 mm^2 for all sheep (P1–P9). The average values of the individual animals are provided in Table 3.

On the stent side, the analysis was carried out depending on the animal groups and thus the different periods of stent insertion. The average lumen of all evaluated slices from cutting sections A–E of the stent was 2.3 mm^2 for animals P7–P9 (implanted for 3 months). When focusing on the parts B, C and D of the actual stent, values were 2.53, 4.59, and 1.92 mm^2, respectively.
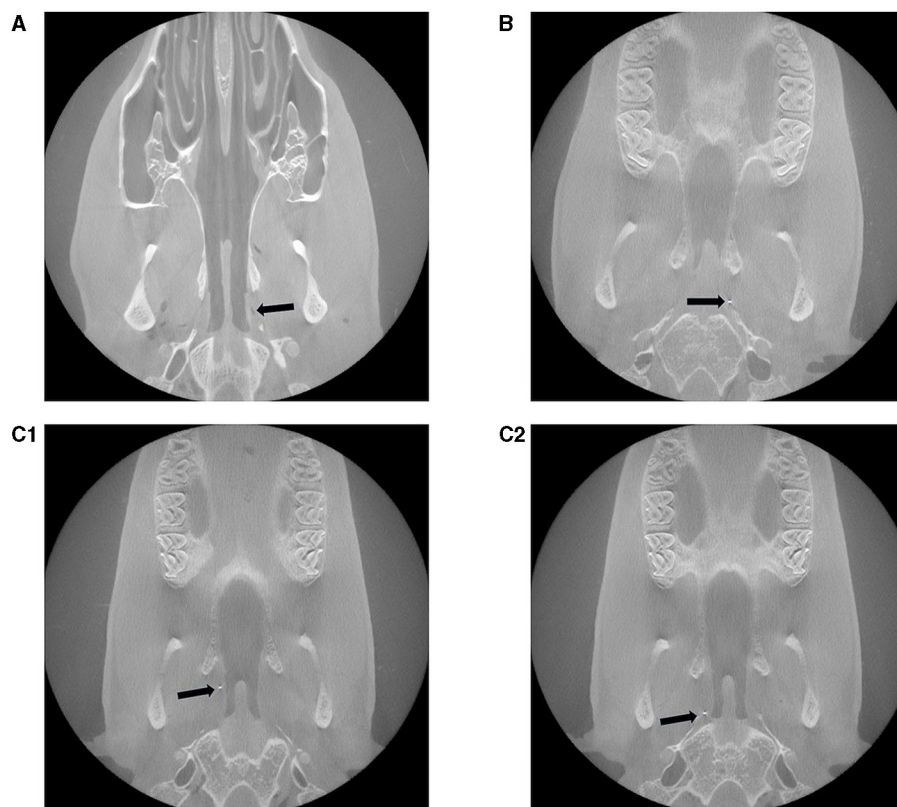
FIGURE 6
Representative post mortem CBCT scans of three different experimental sheep with inserted stent in the ETs. **(A)** Animal P6: no marker, but instead air is visible, **(B)** P1: 1 marker and **(C1, C2)** P8: in total 2 markers are visible. The arrows point to the visible X-ray markers or, in P6, to the air.

The average value across all slices for animal group P4–P6 (implanted for 6 months) was 1.67 mm^2. The average values for the individual cutting sections were 1.76 mm^2 for B, 1.64 mm^2 for C and 1.42 mm^2 for D.

The average value for animal group P1–3 (implanted for 12 months) was 0.99 mm^2. The mean values for the individual cutting sections were 1.12 mm^2 for section B, 1.51 mm^2 for C and 1.07 mm^2 for D. Values for the different stent cutting sections of all animals are provided in Table 4. In most cases, the open lumen was larger in the central part of the stent (section C). Furthermore, average values for the animal groups appeared to be larger in section B compared to section D. Additionally, in all animals except P6, the measured tubal lumen area in the non-stented section E was smaller than in section A, the non-stented area of the pharyngeal side.

Regarding the amount of secretion in the tubal lumen, the average value for the control slices of all animals P1–P9 was 0.16 mm^2, resulting in an average free lumen of 0.63 mm^2.

On the stent side, the cutting sections of all slices A–E for each animal were averaged and shown with the values for the tubal lumen (Figure 8). The mean values for the animal groups were then calculated based on these values. For the P7–P9 group, the average value for secretion was 1.38 mm^2. This resulted in a free volume of 0.92 mm^2. For the group P4–P6 the mean area covered by secretion was 0.80 mm^2. This resulted in a free volume of 0.87 mm^2. For the animal group

P1–P3 the mean value was 0.42 mm^2 and a free volume of 0.57 mm^2.

The areas of the stents present in cutting sections B–D were evaluated and averaged over the length of the stent (Figure 9). The mean value was then calculated for each animal group. The average value for P7–P9 was 3.19 mm^2, for P4–P6 it was 1.91 mm^2, and for P1–P3 it was 0.95 mm^2. As the duration of the experiment increased, the stent lumen became smaller.

The number of struts counted in total in cutting sections B–D averaged 101 for P7–P9, 75 for P4–P6 and 62 for P1–P3. Thus, a reduction in the number of visible struts could be seen as the observation time increased. The values of the free struts in the lumen were on average 36, 7, and 9 free struts, respectively.

The epithelial score on the control side showed values of 1.9 for animals P1–P3, 1.8 for P4–P6 and 2 for P7–P9 when averaging all slices for each animal and then for the animal groups. Overall, the mean value on the control side was 1.9.

On the stent side, a quadrant division was made in cutting sections B–D (compare Figure 3B). For each animal, three slices per section were evaluated resulting in a maximum of 12 values per stent section. Table 5 summarizes the results for each animal for cutting sections B, C, and D.

For the animal group P7–P9, averaging all evaluated slices of cutting section B resulted in a score of 2.25. For section C, this was 2.39 and for section D 2.3. For the animal group P4–P6, there was
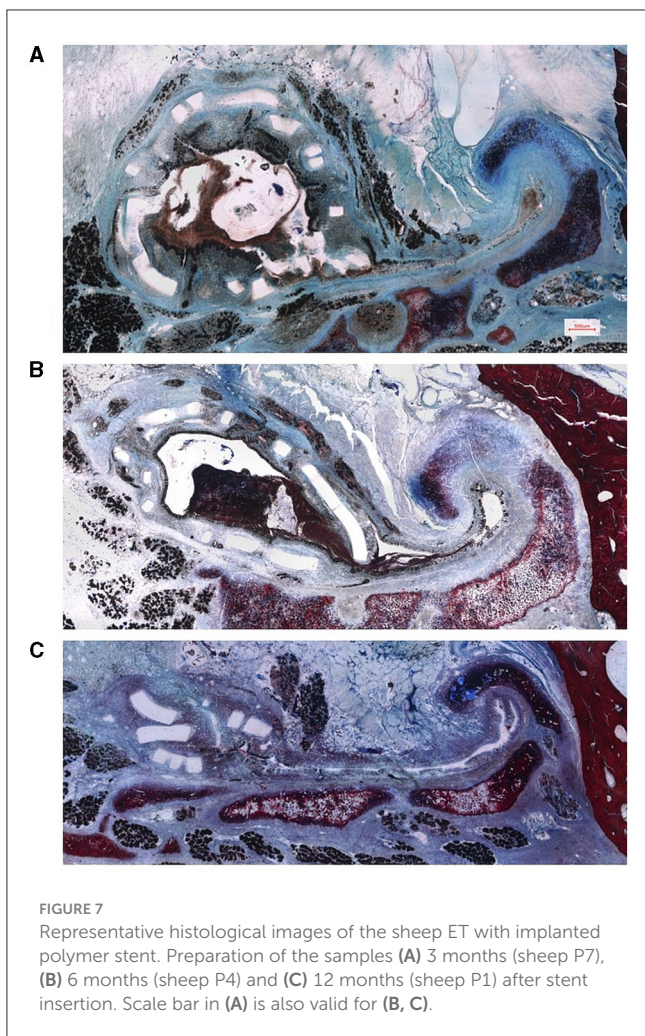
FIGURE 7
Representative histological images of the sheep ET with implanted polymer stent. Preparation of the samples **(A)** 3 months (sheep P7), **(B)** 6 months (sheep P4) and **(C)** 12 months (sheep P1) after stent insertion. Scale bar in **(A)** is also valid for **(B, C)**.

TABLE 3 Area of average ET lumen (L) (mm^2) on control sides for each sheep.

Sheep (control side)	ET lumen (mm^2) − average value
P1	0.48
P2	0.39
P3	0.60
P4	0.71
P5	1.04
P6	1.32
P7	0.69
P8	1.51
P9	0.44

$N = 3$ for each sheep (P1–P9).

TABLE 4 Average values of the ET lumen for each sheep (P1−9) for cutting sections B, C, and D.

Sheep	ET lumen section B (mm^2)	ET lumen section C (mm^2)	ET lumen section D (mm^2)
P1	0.25	0.24	0.20
P2	1.15	1.36	1.24
P3	1.96	2.93	1.78
P4	1.07	2.99	2.29
P5	3.00	0.90	0.72
P6	1.22	1.04	1.26
P7	2.74	4.17	1.39
P8	2.27	5.11	2.67
P9	2.59	4.47	1.68

$N = 3$ per section and sheep.

a mean value of 2.07 for section B and 2.0 for cutting sections C and D. In animals P1–P3, mean values were 2, 2.17 and 2.21 for cutting sections B, C, and D, respectively. It was noticeable that after 3 months of stent insertion (P7–P9) values tended to be higher and thus the epithelial quality appeared worst in comparison.

4 Discussion

Eustachian tube dysfunction can cause inadequate ventilation of the middle ear and is therefore one of the main reasons for the development of chronic middle ear infections. Depending on the patient's case, permanent support of the ET is not always necessary, but rather temporary support for the ET. Therefore, biodegradable stents are under development. The purpose of the current study was to investigate feasibility of implantation and degradation kinetics of biodegradable polymer stents in the ET. The study was set up as an orientation study. The reason for this procedure with a small number of animals but three different observation periods was that there was insufficient advance information on the behavior and possible degradation of the polymer stents in the ET. Due to the small number of experimental animals (N

FIGURE 8
Average values of the ET lumen area and secretion (mm^2) for each sheep (P1−P9) for cutting sections A−E. $N = 15$ (five parts with three slices each) except for P4 ($N = 10$) and P9 ($N = 14$) because the tube lumen was not fully shown on the slices.

$= 3$ per observation period), presentation of results could only be descriptive.

Due to the anatomical characteristics similar to humans, the large animal model blackface sheep was chosen. Especially the

dimensions of the ET of blackface sheep match the anatomically dimensions in human (Miller et al., 2014). Earlier studies have already shown that *in vivo* stent implantation into the ET in sheep and porcine models were possible (Pohl et al., 2018; Kang et al., 2022b) and that stenting the ET was well tolerated in sheep (Pohl et al., 2018).

These findings were confirmed in this experiment for the used biodegradable stent prototype made from PLLA. All sheep showed overall good tolerability of the stents and there were no behavioral problems at any time. All stents were positioned in the cartilaginous part of the ET and the fact that the pharyngeal ET orifices of all sheep were closed at half-time and final follow-ups indicates that besides minimal opening right after stent placement no patulous ET was induced.

Controlling middle ear ventilation by tympanometry, most sheep showed physiological tympanograms. Only two animals had ventilation problems lasting several weeks (P3, P6). The other animals only experienced sporadic disturbances (curve type B or C). These sporadic disturbances were observed to a comparable extent in implanted and not implanted control tubes. Therefore, these have to be considered "normal" in sheep and cannot be attributed to stent implantation.

There might be several potential reasons for these sporadic deviations. Tympanometric measurements could be influenced by earwax (Pohl et al., 2017). Despite regular rinsing, mechanical cleaning was necessary during GA after initial cleaning in several animals due to earwax accumulation. Especially in animal P6 more frequent mechanical cleaning on the stented side was necessary.

FIGURE 9
Areas of the stents in cutting sections B−D for each sheep (P1−9). $N = 9$ (three parts with three slices each) except for P1, P2, P3 ($N = 8$) and P6 ($N = 6$) due to too few struts.

Furthermore, incorrect measurements could also occur due to a lack of cooperation, swallowing or movement artifacts. Sporadic occurrence of type C curves may also be caused by short-term pressure shifts, which are non-pathologic (Pohl et al., 2017). In general, all these possible explanations should affect both sides in a comparable manner. Due to the small number of animals per group, the measured disturbances in middle ear ventilation cannot safely be attributed to stent placement. This question has to be addressed in future tests with larger numbers of animals.

The current study deals with biodegradable stents for the ET. There is only one other study known that investigated biodegradable stents in the ET (Kang et al., 2023). In that study, magnesium stents were investigated in a porcine model in just two animals. It appeared to be safe, but biodegradation already occurred within 2 weeks (Kang et al., 2023). Therefore, despite their good biocompatibility, only brief support of the ET would be possible, which in our opinion would be too short to support middle ear ventilation and healing of OME. Based on their own experience, our involved surgeons suggested a period of 3 months as time the ET needs support even though no justifying reference was given. Due to the different nature of ETD, patients will probably need support of ET function for different durations. Unfortunately, also diagnostic methods for the reasons of ETD are limited (Oppel et al., 2022b). Therefore, support of ET function for 3 months should be seen as starting point that could help most patients needing a non-permanent support to avoid possible chronification of symptoms.

In the current study, stents made from PLLA were used and have shown support of ET for at least 3 months. Even afterwards, enlarged ET lumina were detected compared to the control side. Therefore, the current findings on degradation kinetics appear promising and consistent with the temporal requirements of supporting the ET.

There is already a multitude of other studies examining the degradation of polymer stents used for various medical purposes. Tubular poly (PCL/PLGA) ureteral stents were tested in ureteral obstruction in six pigs (Wang et al., 2015). All of them had degraded by 10 weeks post insertion with no ureteral obstruction (Wang et al., 2015). Clinical studies of everolimus eluting PLLA stents showed mechanical support during the first 3 months of implantation (Beshchasna et al., 2020). Studies of PLLA biodegradable stents in the gastrointestinal tract showed degradation due to hydrolysis after 4–5 weeks and dissolved during a period of 2–3 months (Kang, 2019). Compared to these published studies, degradation of the tested polymeric ET stent appeared to
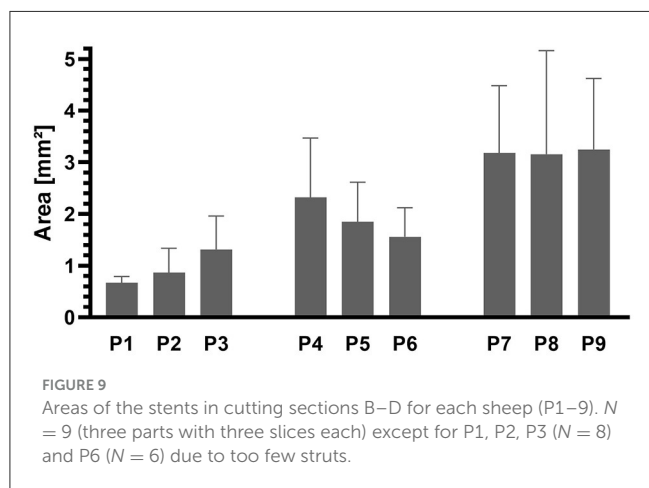
TABLE 5 Number of appearance of scores 1 to 4 in different animals and stent regions.

	P1 B/C/D	P2 B/C/D	P3 B/C/D	P4 B/C/D	P5 B/C/D	P6 B/C/D	P7 B/C/D	P8 B/C/D	P9 B/C/D
1	–/–/–	2/–/1	2/1/3	1/6/–	–/1/–	–/–/–	–/–/–	7/–/–	–/–/–
2	–/–/–	10/9/6	7/10/6	11/5/12	9/5/4	4/12/12	3/8/4	5/11/–	5/3/12
3	–/–/–	–/2/5	2/1/2	–/1/–	3/6/–	–/–/–	9/4/8	–/1/–	7/9/–
4	–/–/–	–/1/–	1/–/1	–/–/–	–/–/–	–/–/–	–/–/–	–/–/–	–/–/–

Mostly N = 36 per animal (nine slices with four values each). Evaluation could not be done in terms of quadrants in P1 as ET was already collapsed.

be slower. Three months after implantation, first degradation or fragmentation was seen. After 12 months, the stents were collapsed but not completely dissolved. When analyzing the degradation kinetics, it has to be taken into account that not only the material properties but also the stent structure, size and surrounding environment have a substantial influence on the degradation (Kang, 2019). In the ET, the stent is positioned at an air-tissue interface, which could slow down degradation as also reported for Mg stents (Kang et al., 2023).

After 3 months of implantation, the cross-sectional shape of the stent was still round, even though first disarranged struts were found. The strut arrangement deviated significantly from the original shape after 6 months of stent insertion. Struts could also be found in the 12 months stented animals. As time went on, support for ET decreased to the point of collapse. Regarding the collapsed stents, the reasons could be degradation of the material or may be fragmentation due to mechanical load of the stent. Images (like Figure 10) indicate that entire fragments have moved and therefore parts of the stent may no longer be where they were originally located. It is possible that the length over which the stent extended within the ET at the time of embedding also changed compared to the original stent. In addition, the stents were implanted in a functional, undisturbed ET. In the intended later application in patients, the stent shall re-open dysfunctional ETs. It still remains unknown whether the stent would be able to restore ventilation of the middle ear in these cases and how the condition would affect the time the stent keeps its round shape before degradation or collaps.

CBCT scans after euthanasia showed that in most cases at least one of the two X-ray markers was lost during the experimental period. According to the position of the remaining marker, it is assumed that the X-ray marker close to the nasopharyngeal tube entrance was lost. Several conceivable reasons for this are existing. It might be that the X-ray markers were not sufficiently attached to the stent. Another possible explanation may be the stress on the stent because of the physiological movements during natural opening of the ET. The cartilaginous part of the ET in humans opens at least every 1–2 min when yawning, swallowing and moving, thus leading to gas exchange (Smith et al., 2019). Most of the time this happens involuntarily (Smith et al., 2019). In sheep as ruminating animals, even more natural openings of the ET can be expected per day compared to humans. The tensor veli palatini muscle plays a major role in opening the ET. It triggers the opening when contracted (Goulioumis et al., 2022). The muscle arises from the scaphoid fossa and the spina angularis of the sphenoid but also from the lateral wall of the ET cartilage (Goulioumis et al., 2022). Due to these circumstances, it is suspected that adjacent anatomical structures and physiological muscle contractions may cause stress to be exerted on the stent and therefore also on the X-ray markers. These movements could be less pronounced close to the isthmus region of the ET.

This in turn could also explain a larger fragmentation of the stent at its pharyngeal side compared to its isthmus-facing part. If fragmentation would also be the reason for the loss of function after more than 3 months of implantation, parts of the stent including the proximal X-ray marker could also be simply washed out of the ET. At least for the Mg stent it was assumed that residual struts were flushed into the nasopharynx with the nasal mucus (Kang et al., 2023).
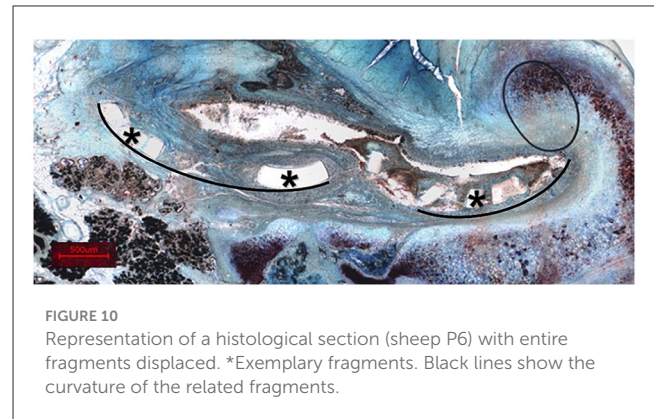

FIGURE 10
Representation of a histological section (sheep P6) with entire fragments displaced. *Exemplary fragments. Black lines show the curvature of the related fragments.

The initial positioning of the stent could have an impact on the type of force exerted on the stent and thus on the subsequent movement and the degradation of the stent. As all stents in the study were comparably positioned (no stent entered the isthmus and all pharyngeal orifices were closed at the controls), it may be speculated that variability in position should not have a major influence on results in the current study.

In this study it was noticed that the epithelium even on the control side was not fully intact (rating 1.9). Based on this fact, it can be stated that epithelial damage on the stent side (rating approximately 2.1) is compromised not only due to stent insertion, as the control side does not perform much better. It is known that histological preparation can influence the quality of the slices (Rolls, 2012). Therefore, it is suspected that damage to the epithelium may have occurred during embedding. Thus, only a slight reduction in epithelial quality can be attributed to the stent.

Even if not statistically proven, the study indicated that the stent supports the ET for at least 3 months when implanted in an ET without ETD. The results can serve as initial assessment and provide the basis for further investigations.

5 Conclusion

The implantation of biodegradable polymer stents into the ET to support ventilation of the middle ear has been successfully proven. Positioning of the stent in the ET was reliable without generating a patulous ET. The stent in its present form seems to fully support the ET for at least 3 months, even though first indication of degradation or fragmentation was found and this is based on only three animals. After 6 months of implantation the stents were partly collapsed and after 12 months, the shape of the ET was similar to the not implanted sides but with remainders of struts in the tissue. With the current prototype, the intended 3 months of support appear to be provided before the stent loses functionality. Thus, extended animal trials with this stent seem to be justified.

Data availability statement

The original contributions presented in the study are included in the article/Supplementary material, further inquiries can be directed to the corresponding authors.

Ethics statement

Author contributions

Funding

Acknowledgments

Conflict of interest

The authors declare that the research was conducted in the absence of any commercial or financial relationships that could be construed as a potential conflict of interest.

Publisher's note

All claims expressed in this article are solely those of the authors and do not necessarily represent those of their affiliated organizations, or those of the publisher, the editors and the reviewers. Any product that may be evaluated in this article, or claim that may be made by its manufacturer, is not guaranteed or endorsed by the publisher.

Supplementary material

The Supplementary Material for this article can be found online at: https://www.frontiersin.org/articles/10.3389/fauot.2024.1414831/full#supplementary-material

References

Ailianou, A., Ramachandran, K., Kossuth, M. B., Oberhauser, J. P., and Kornfield, J. A. (2016). Multiplicity of morphologies in poly (l-lactide) bioresorbable vascular scaffolds. *Proc. Natl. Acad. Sci. U.S.A.* 113, 11670–11675. doi: 10.1073/pnas.1602311113

Bal, R., and Deshmukh, P. (2022). Management of eustachian tube dysfunction: a review. *Cureus* 14:e31432. doi: 10.7759/cureus.31432

Beshchasna, N., Saqib, M., Kraskiewicz, H., Wasyluk, Ł., Kuzmin, O., Duta, O. C., et al. (2020). Recent advances in manufacturing innovative stents. *Pharmaceutics* 12:349. doi: 10.3390/pharmaceutics12040349

Di Martino, E., Thaden, R., Krombach G. A., and Westhofen, M. (2004). Function tests for the Eustachian tube. Current knowledge. *HNO* 52, 1029–1039. doi: 10.1007/s00106-004-1152-7

Federov, A., Beichel, R., Kalpathy-Cramer, J., Finet, J., Fillion-Robin, J., Pujol, S., et al. (2012). 3D Slicer as an image computing platform for the quantitative imaging network. *Magn. Reson. Imaging* 30, 1323–1341. doi: 10.1016/j.mri.2012.05.001

Gelfand, S. A. (2016). *Essentials of Audiology.* Stuttgart: Thieme Medical Publishers. doi: 10.1055/b-006-161125

Goulioumis, A. K., Gkorpa, M., Athanasopoulos, M., Athanasopoulos, I., and Gyftopoulos, K. (2022). The Eustachian tube dysfunction in children: anatomical considerations and current trends in invasive therapeutic approaches. *Cureus* 14:e27193. doi: 10.7759/cureus.27193

Healy, G. B., and Rosie, K. W. (2003). "Otitis media and middle ear effusions" in *Ballenger's Otorhinolaryngology - Head and Neck Surgery*, eds. J. J. Ballenger, and J. B. Snow (Hamilton, ON: BC Decker Inc.), 249–260.

Hu, T., Yang, C., Lin, S., Yu, Q., and Wang, G. (2018). Biodegradable stents for coronary artery disease treatment: recent advances and future perspectives. *Mater. Sci. Eng. C. Mater. Biol. Appl.* 91, 163–178. doi: 10.1016/j.msec.2018.04.100

Kang, J. M., Kim, S. H., Choi, Y. J., Park, Y., Ryu, D. S., Kang, W. S., et al. (2022a). Sirolimus-eluting cobalt-chrome alloy stent suppresses stent-induced tissue hyperplasia in a porcine Eustachian tube model. *Sci Rep.* 12:3436. doi: 10.1038/s41598-022-07471-2

Kang, J. M., Kim, S. H., Ryu, D. S., Park, Y., Won, D., Kim, J. W., et al. (2022b). Tapered self-expandable metallic stent optimized for Eustachian tube morphology in a porcine ET model. *Sci. Rep.* 12:20290. doi: 10.1038/s41598-022-24615-6

Kang, J. M., Kim, S. H., Ryu, D. S., Park, Y., Won, D., Kim, J. W., et al. (2023). Preliminary results of absorbable magnesium stent for treating Eustachian tube dysfunction in a porcine model. *PLoS ONE* 18:e0284584. doi: 10.1371/journal.pone.0284584

Kang, Y. (2019). A review of self-expanding esophageal stents for the palliation therapy of inoperable esophageal malignancies. *Biomed. Res. Int.* 2019:9265017. doi: 10.1155/2019/9265017

Miller, F., Burghard, A., Salcher, R., Scheper, V., Leibold, W., Lenarz, T., et al. (2014). Treatment of middle ear ventilation disorders: sheep as animal model for stenting the human Eustachian tube – a cadaver study. *PLoS ONE* 9:e113906. doi: 10.1371/journal.pone.0113906

Oppel, N., Ezzat, M., Krüger, P., Schmitt, K., Napp, A., Pohl, F., et al. (2022a). Development of an *in vivo* model for Eustachian tube dysfunction. *Bioengineering* 9:317. doi: 10.3390/bioengineering9070317

Oppel, N., Paasche, G., Bleich, A., Lenarz, T., and Schuon, R. (2022b). Intravascular ultrasonography (IVUS)—a tool for imaging the eustachian tube? *Bioengineering* 9:733. doi: 10.3390/bioengineering9120733

Poe, D. S., Grimmer, J. F., and Metson, R. (2007). Laser Eustachian tuboplasty: two-year results. *Laryngoscope* 117, 231–237. doi: 10.1097/01.mlg.0000246227.65877.1f

Pohl, F., Paasche, G., Lenarz, T., and Schuon, R. (2017). Tympanometric measurements in conscious sheep - a diagnostic tool for pre-clinical middle ear implant studies. *Int. J. Audiol.* 56, 53–61. doi: 10.1080/14992027.2016.1227480

Pohl, F., Schuon, R. A., Miller, F., Kampmann, A., Bültmann, E., Hartmann, C., et al. (2018). Stenting the Eustachian tube to treat chronic otitis media - a feasibility study in sheep. *Head Face Med.* 14:8. doi: 10.1186/s13005-018-0165-5

Rolls, G. O. (2012). *Schnittprobleme und mögliche Lösungen - Nachbearbeitung schwieriger Gewebeblöcke.* Available at: https://www.biosystems.ch/servefile/?encdlof=qTv4Imd-T4aZf3XAHav6P3FAJj9yLeA4RzQg2oILprnMrItyg8TAsQFNH4fwXfCixtZlHsx-xYEob8evGmVDxQandct= (accessed March 20, 2024).

Rosenbusch, L., Schuon, R., Wilfling, T., Krüger, P., Lebahn, K., John, S., et al. (2023). Investigation of stent prototypes for the eustachian tube in human donor bodies. *Bioengineering* 10:743. doi: 10.3390/bioengineering10060743

Schilder, A. G. M., Bhutta, M. F., Butler, C. C., Holy, C., Levine, L. H., Kvaerner, K. J., et al. (2015). Eustachian tube dysfunction: consensus statement on definition, types, clinical presentation and diagnosis. *Clin.Otolaryngol.* 40, 407–411. doi: 10.1111/coa.12475

Schrom, T., Kläring, S., and Sedlmaier, B. (2007). Treatment of chronic tube dysfunction. Use of the tube conductor. *HNO* 55, 871–875. doi: 10.1007/s00106-007-1539-3

Schümann, K., Röhr, U., Grabow, N., and Schmitz, K. (2016). *Expandierbare Struktur.* Patent No DE102016117398B4. Munich: Deutsches Patent und Markenamt.

Schümann, K., Wilfling, T., Paasche, G., Schuon, R., Schmidt, W., Müller, H., et al. (2018). Development of biodegradable stents for the treatment of Eustachian tube dysfunction. *Curr. Direct. Biomed. Eng.* 4, 505–508. doi: 10.1515/cdbme-2018-0121

Schümann, K., Wilfling, T., Paasche, G., Schuon, R., Tautorat, C., Schmitz, K., et al. (2020). Polymeric stents for the Eustachian tube: development and human cadaver study. *Curr. Direct. Biomed. Eng.* 6:20203054. doi: 10.1515/cdbme-2020-3054

Silvola, J., Kivekäs, I., and Poe, D. S. (2014). Balloon dilation of the cartilaginous portion of the eustachian tube. *Otolaryngol–Head Neck Surg.* 151, 125–130. doi: 10.1177/0194599814529538

Smith, M. E., Bance, M. L., and Tysome, J. R. (2019). Advances in Eustachian tube function testing. *World J Otorhinolaryngol Head Neck Surg.* 5, 131–136. doi: 10.1016/j.wjorl.2019.08.002

Sudhoff, H., Schröder, S., Reineke, U., Lehmann, M., Korbmacher, D., Ebmeyer, J., et al. (2013). Therapy of chronic obstructive Eustachian tube dysfunction: evolution of applied therapies. *HNO* 61, 477–482. doi: 10.1007/s00106-013-2691-6

Teixeira, M. S. (2020). Understanding Eustachian tube function. *Braz. J. Otorhinolaryngol.* 86, 523–524. doi: 10.1016/j.bjorl.2020.02.001

Wang, X., Shan, H., Wang, J., Hou, Y., Ding, J., Chen, Q., et al. (2015). Characterization of nanostructured ureteral stent with gradient degradation in a porcine model. *Int. J. Nanomedicine* 10, 3055–3064. doi: 10.2147/IJN.S80810

Williams, B., Taylor, B. A., Clifton, N., and Bance, M. (2016). Balloon dilation of the Eustachian tube: a tympanometric outcomes analysis. *J. Otolaryngol. Head Neck Surg.* 45:13. doi: 10.1186/s40463-016-0126-6